Supplementary Information

Proinflammatory role of histamine-releasing factor in mouse models of asthma and allergy

Jun-ichi Kashiwakura, Tomoaki Ando, Kenji Matsumoto, Miho Kimura, Jiro Kitaura, Michael H. Matho, Dirk M. Zajonc, Tomomitsu Ozeki, Chisei Ra, Susan M. MacDonald, Reuben P. Siraganian, David H. Broide, Yuko Kawakami, and Toshiaki Kawakami

Content

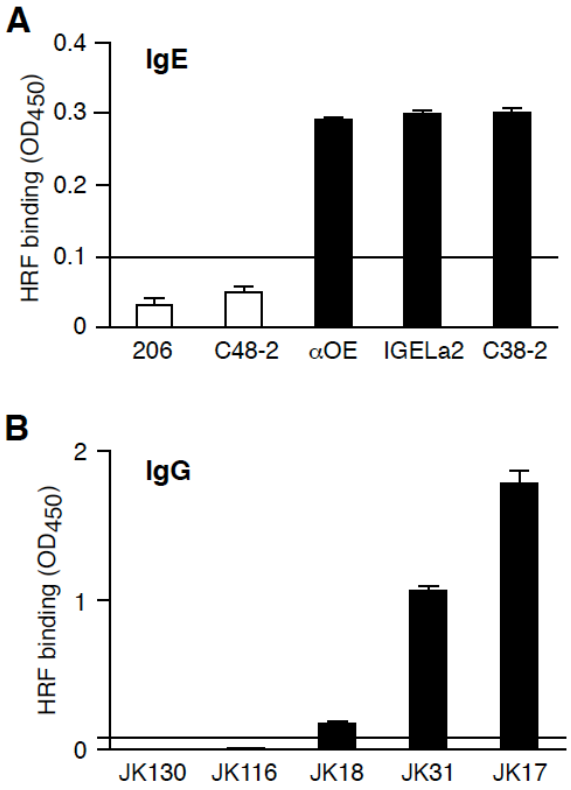

Figure S1. GST-mHRF-reactive IgE and IgG molecules bind mHRF-His_6 as well. mHRF-His_6 was coated onto a 96-well plate. After blocking with 1% BSA-PBS, the plate was incubated with 10 μg/ml IgE (**A**) and IgG (**B**) molecules for 3 h. HRF-bound IgE molecules were detected by incubation with biotin-conjugated anti-mouse IgE followed by SA-HRP, and HRF-bound IgG molecules were detected with HRP-conjugated anti-mouse IgG. Color was developed and detected at 450 nm.

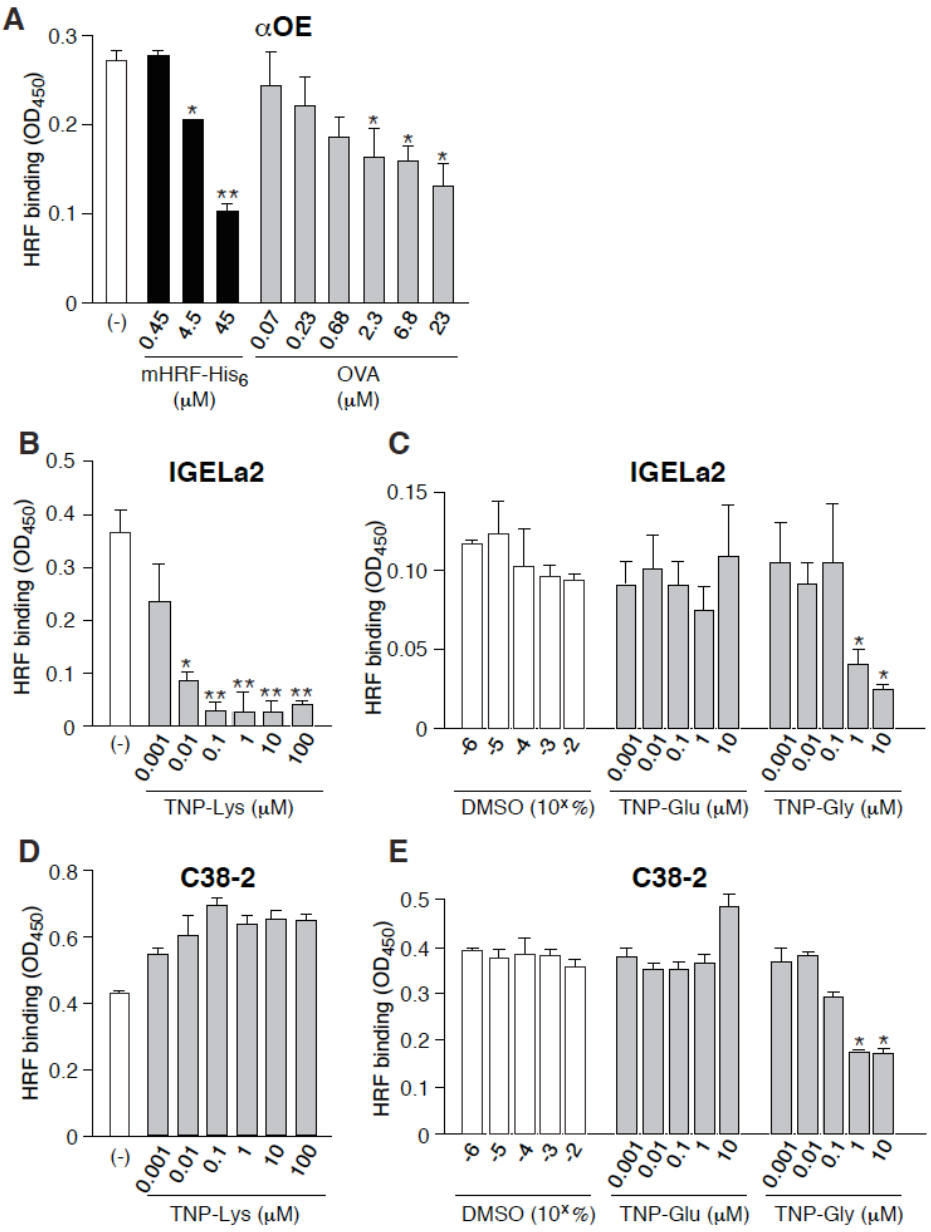

Figure S2. HRF-binding sites of IgEs overlap with their antigen-binding sites. The indicated IgE molecules (10 μg/ml) were incubated in GST-mHRF-coated wells in the presence or absence (-) of the indicated concentrations of competitor. Bound IgEs were detected by incubation with biotin-conjugated anti-mouse IgE antibody, followed by incubation with streptavidin-HRP. The absorbance at 450 nm was measured after development of the color. Data indicate mean ± SEM. Representative of 2 experiments.

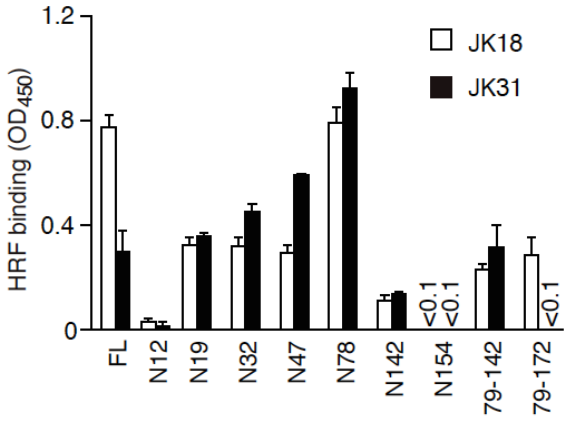

Figure S3. HRF-reactive IgG molecules bind HRF via the N-terminal 19 residue and internal sequences of HRF. The full-length (FL) and truncated GST proteins were coated onto plastic wells. After blocking, JK18 and JK31 IgGs were incubated. The bound IgGs were detected by incubation with HRP-conjugated anti-mouse IgG antibody. The absorbance at 450 nm was measured after development of the color. Data indicate mean ± SEM.

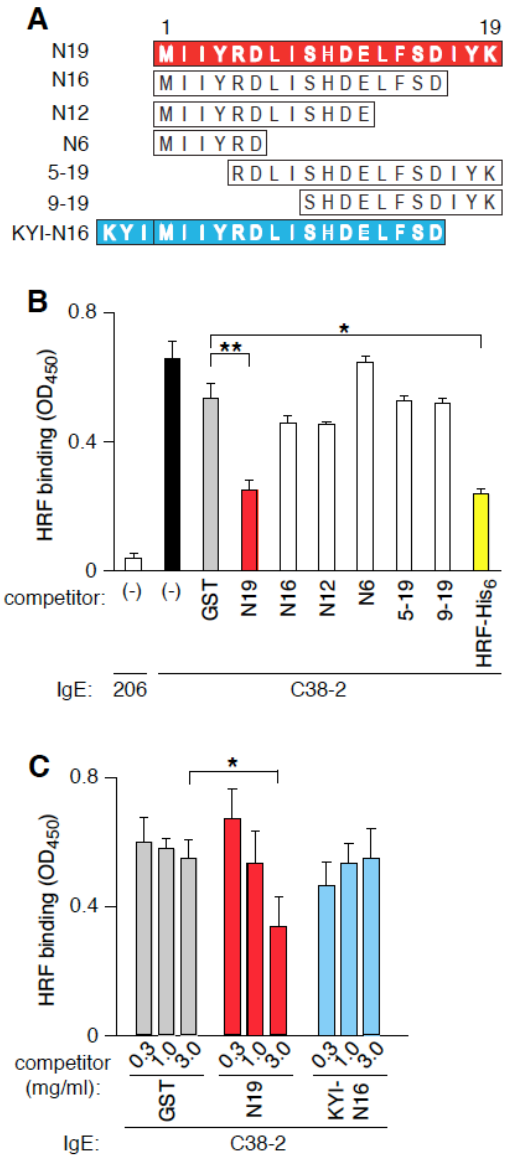

Figure S4. N-terminal shorter peptides or a scrambled peptide do not inhibit HRF-IgE interactions. (**A**) Scheme of GST-mHRF constructs used. KYI-N16 is a construct containing three C-terminal residues, KYI, of N19 in the reverse order placed in front of N16. (**B,C**) mHRF-His_6 was coated onto a 96-well plate. After blocking by 10% FCS, the plate was incubated with the indicated IgE molecules with or without the competitor GST fusion proteins (150 μM in **B**; the concentrations indicated in **C**) for 3 h. HRF-bound IgEs were detected by incubation with biotin-conjugated anti-mouse IgE, followed by streptavidin-HRP. Color was developed and detected at 450 nm. For a positive control, mHRF-His_6 (50 μM) was used. *, **: $p<0.05$, $p<0.01$ by Student's t-test.

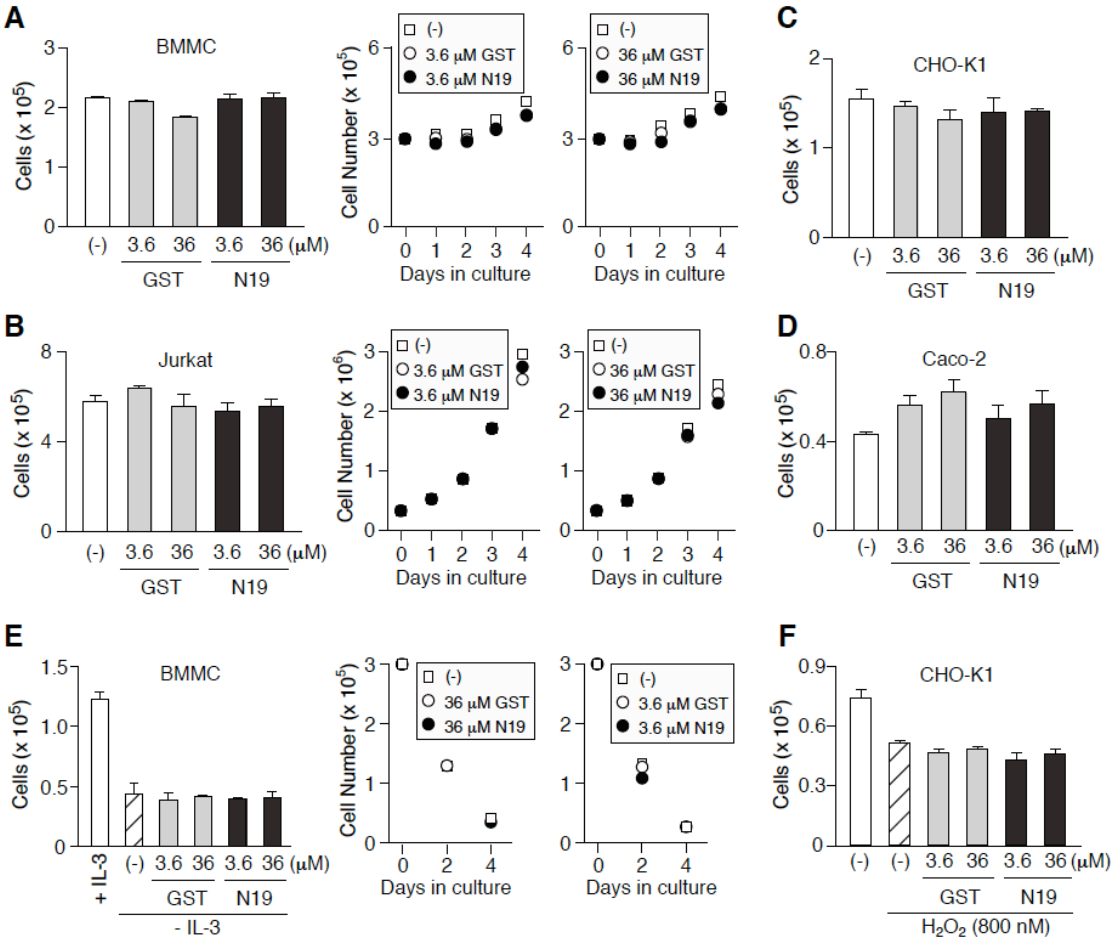

Figure S5. GST-N19 does not affect the growth or apoptosis in various cells. (**A-D**) The indicated cells were cultured in the absence (-) or presence of the indicated concentrations of GST or GST-N19 for 2 (bar graphs) or 4 (time course) days, and live cells were counted in the presence of Trypan blue. Data indicate mean ± SEM. Representative of 2 experiments. Note that error bars are omitted in the time course data. There were no statistically significant differences at any time points. (**E,F**) Apoptosis was induced by IL-3 depletion in BMMCs for 3 (left) or 4 (right) days and by 800 nM H_2O_2 in CHO-K1 cells for 2 days, and live cells were counted. Data indicate mean ± SEM. Representative of 2 experiments. There were no statistically significant differences at any time points.

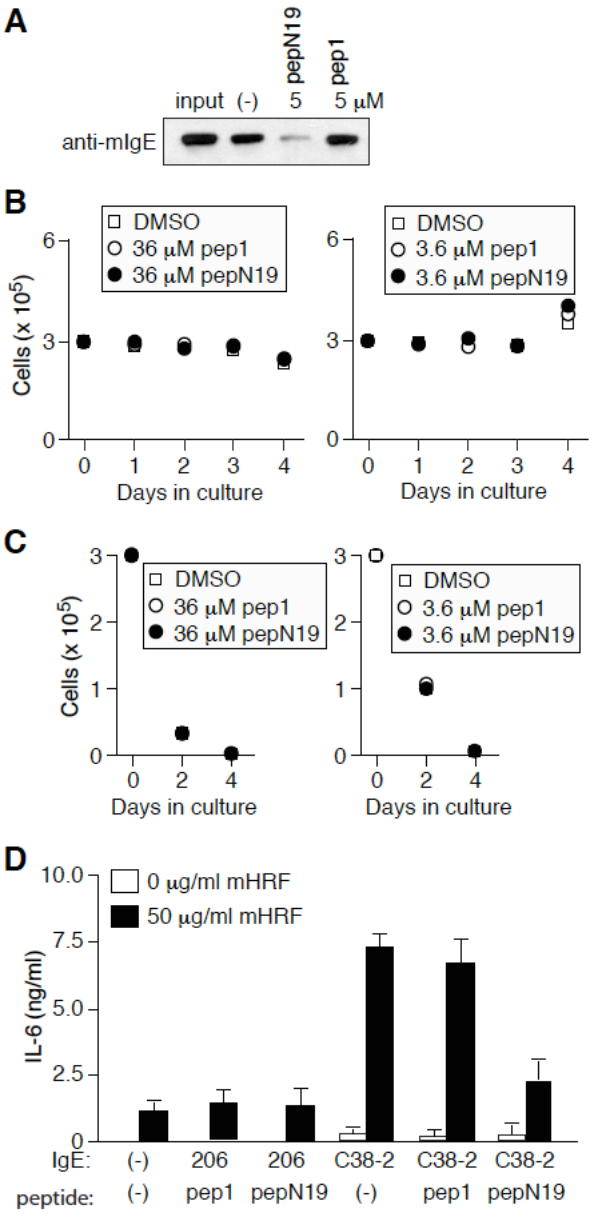

Figure S6. Inhibition of HRF-IgE interactions and HRF + IgE-induced mast cell activation by the synthetic N19 peptide (pepN19). (**A**) Inhibition of HRF-IgE interactions by pepN19. C38-2 IgE was incubated with GST-mHRF-agarose beads in the absence (-) or presence of the indicated peptides. Pep1 was a control peptide. Beads-bound IgE was pulled down and detected by immunoblotting. (**B**) Effect of pepN19 on the growth of BMMCs. (**C**) Effect of pepN19 on growth factor deprivation-induced apoptosis in BMMCs. (**D**) BMMCs were incubated with mHRF-His_6 and the indicated IgE in the absence or presence of 40 μM pepN19 or a control peptide (pep1: KYIDSFLEDHSILDRYIIM) for 20 h for the measurement of secreted IL-6.

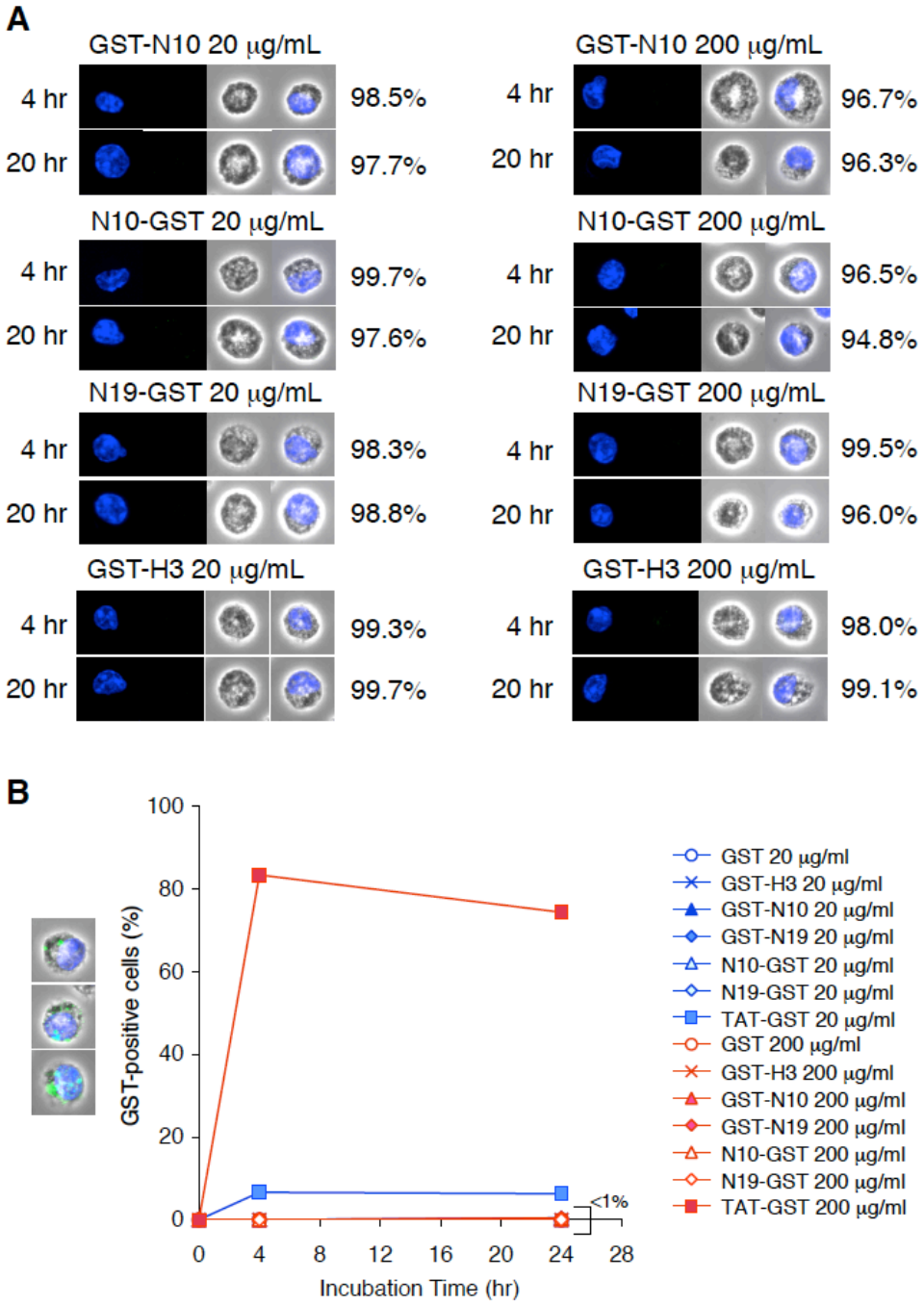

Figure S7. Neither GST-N19 nor GST-H3 enters a mast cell. BMMCs were incubated with the indicated GST fusion proteins for the indicated periods of time. Washed cells were fixed, permeabilized and stained with anti-GST followed by Alexa Fluor 488-conjugated anti-mouse IgG. Nuclei were stained with DAPI. (**A**) Fluorescence was observed by confocal microscopy. DIC, differential interference contrast image. Original magnification, x150. Percentages of the representative images are shown by scoring ≥150 cells. See **Figure 4A** as well. Representative of 3 experiments. (**B**) Percentages of GST-positive cells similar to the representative merged images (*Left*) are plotted as a function of incubation time. Unlike TAT-GST, no other GST fusions entered the cells in significant amounts.

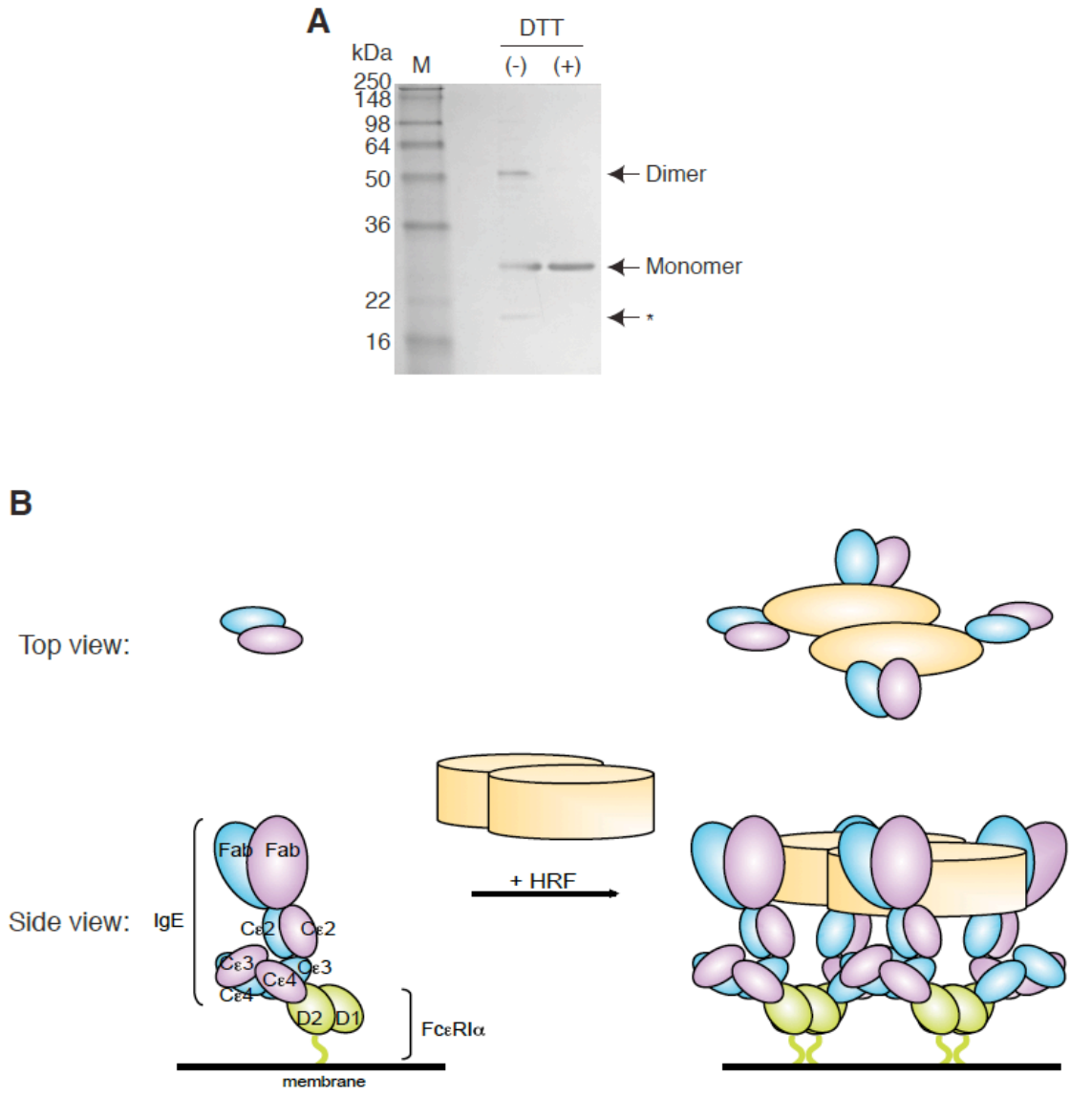

Figure S8. Dimerization of recombinant mHRF and a working model of HRF-mediated FcεRI crosslinking. (**A**) mHRF-His_6 protein was analyzed by SDS-PAGE under reducing or non-reducing conditions and stained with Coomassie Brilliant Blue. Protein indicated by asterisk (*) may be an internally disulfide-bonded HRF or a contaminant of the mHRF-His_6 preparation. Representative of 2 experiments. (**B**) Model for HRF-mediated FcεRI crosslinking. IgE binds FcεRI α chain via the interaction between Cε3 and D2 domains (1). HRF can exist as a dimer and one HRF molecule can bind to two molecules of IgE via interactions with the N19 and H3 regions of HRF. The top view (Top) of IgE at the level of Fab and the side view (Bottom) of IgE and IgE-bound FcεRI α chain are shown on the left. After binding of an HRF dimer, four FcεRI α chain-nucleated complexes will be formed (Right). The cytoplasmic portion of FcεRI α as well as β and γ chains of FcεRI are omitted for clarity.

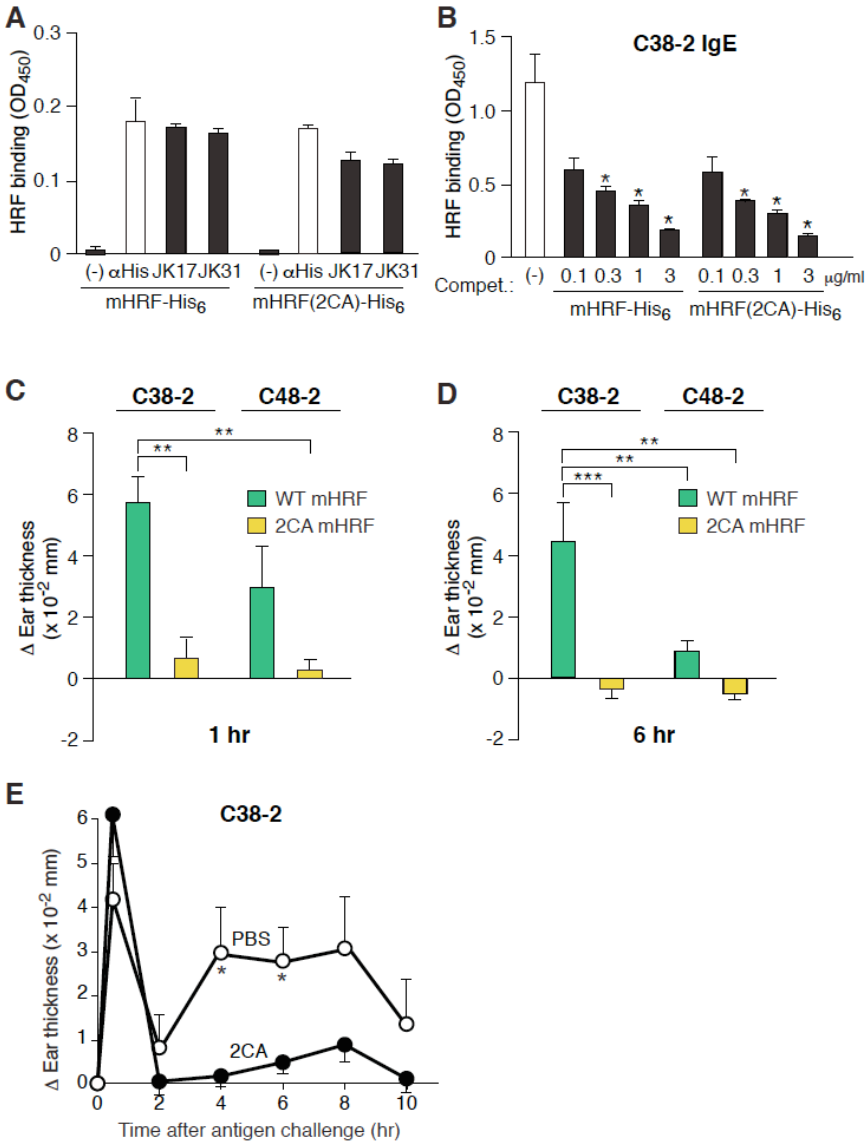

Figure S9. The 2CA mutant mHRF + IgE does not induce PCA despite its reactivity with Igs. (**A,B**) Reactivity of 2CA mutant mHRF with IgG or IgE. (**A**) mHRF-His_6 and mHRF (2CA)-His_6 were immobilized onto ELISA plates in PBS at pH 7.4 and in carbonate buffer at pH 9.5, respectively. Similar immobilization of the capturing agents was confirmed by incubating the plates with anti-His antibody (αHis). Wells coated with mHRF-His_6 and mHRF (2CA)-His_6 were incubated with PBS (-) or HRF-reactive JK17 or JK31 IgGs. Bound IgGs were detected by HRP-conjugated anti-mouse IgG. (**B**) mHRF-His_6 immobilized onto ELISA plates was incubated with C38-2 IgE in the presence of the indicated concentrations of mHRF-His_6 and mHRF (2CA)-His_6. Bound C38-2 IgE was detected with anti-mouse IgE-HRP. Representative of 2 experiments. (**C,D**) Inability of the 2CA mutant of mHRF to induce PCA together with HRF-reactive IgE. PCA was induced by IgE sensitization at the ear followed by intradermal injection of mHRF-His_6 or mHRF (2CA)-His_6. Reactions were quantified by the measurement of ear thickness at 1 h (**C**) and 6 h (**D**). (**E**) C38-2 IgE-sensitized mice were pretreated with PBS or 2CA mHRF-His_6 (100 μg) before injection with mHRF-His_6 (10 μg). PCA reactions were analyzed by measurement of ear thickness. *, **, ***: $p<0.05$, $p<0.01$, $p<0.001$ by Student's t-test.

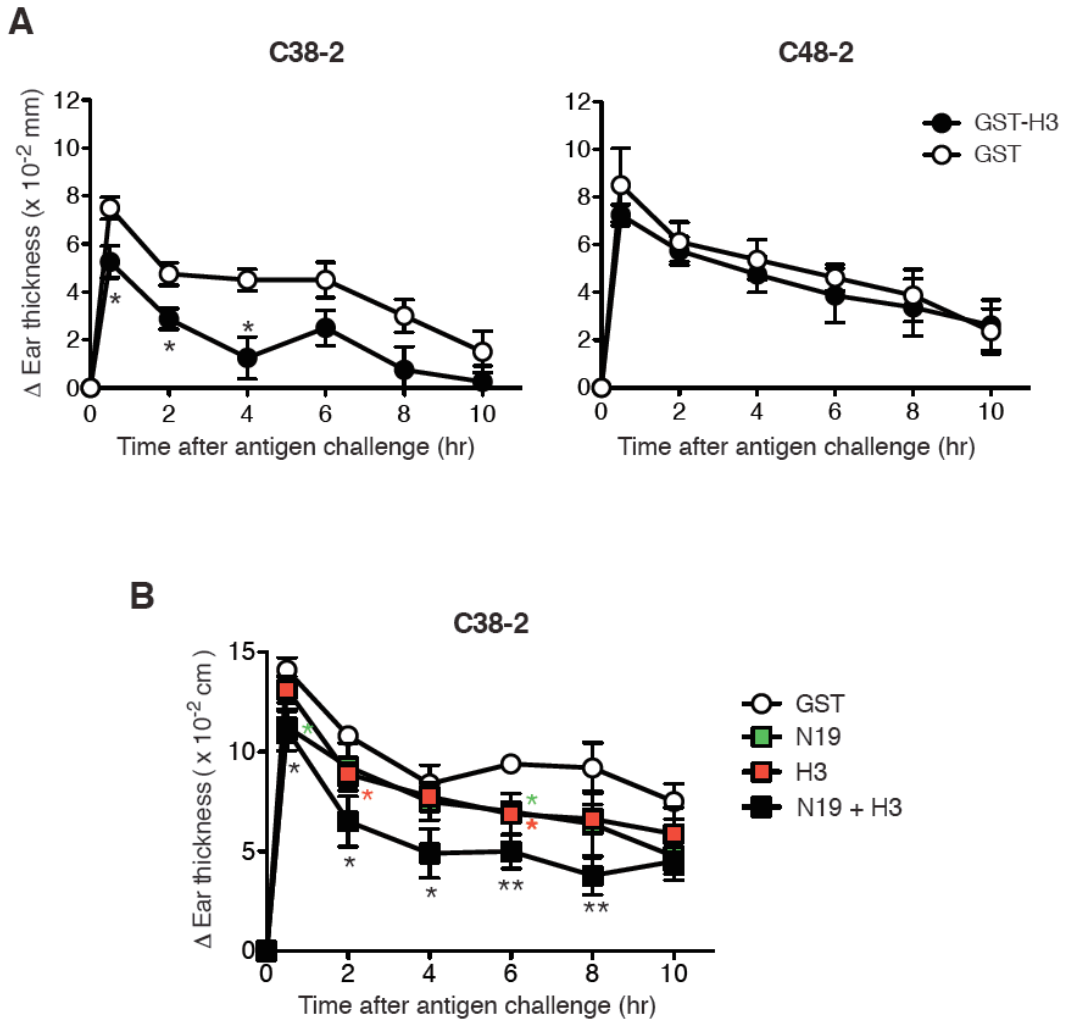

Figure S10. GST-H3 inhibits IgE + antigen-induced PCA and can cooperate with GST-N19 in inhibition of PCA in an additive manner. C38-2 or C48-2 IgE-sensitized mice were intradermally injected with GST or GST-H3 30 min before mHRF-His_6 was injected in C38-2 or C48-2 IgE-sensitized ears. Acute reactions (30 min) and LPR were analyzed by measuring ear thickness. *, **: $p<0.05$, $p<0.01$ vs. GST control.

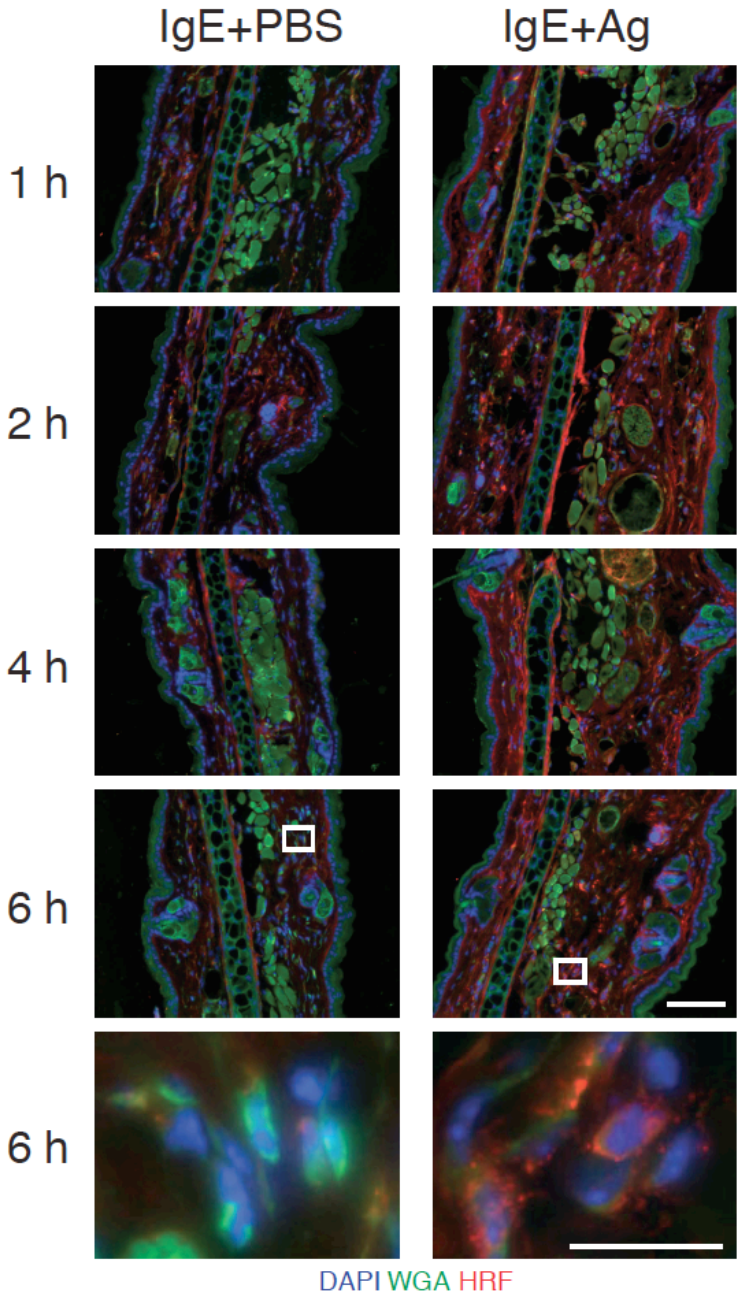

Figure S11. HRF staining is increased in the dermis during late-phase reactions of PCA. Mice were intradermally (i.d.) sensitized with 0.5 μg of C38-2 IgE and i.d. challenged with 100 ng of TNP_{26}-BSA (or PBS as a negative control) at the ears. Immunofluorescence microscopy was performed on paraformaldehyde-fixed, frozen skin sections. HRF was stained red; plasma membranes with wheat germ agglutinin (green); and the nuclei with DAPI (blue). The bar (50 μm) shown in the 6 h, right photo is applied to the low magnification photos in upper 8 panels; the bar (10 μm) is applied to the lowest panels, which are magnified areas of the indicated rectangles.

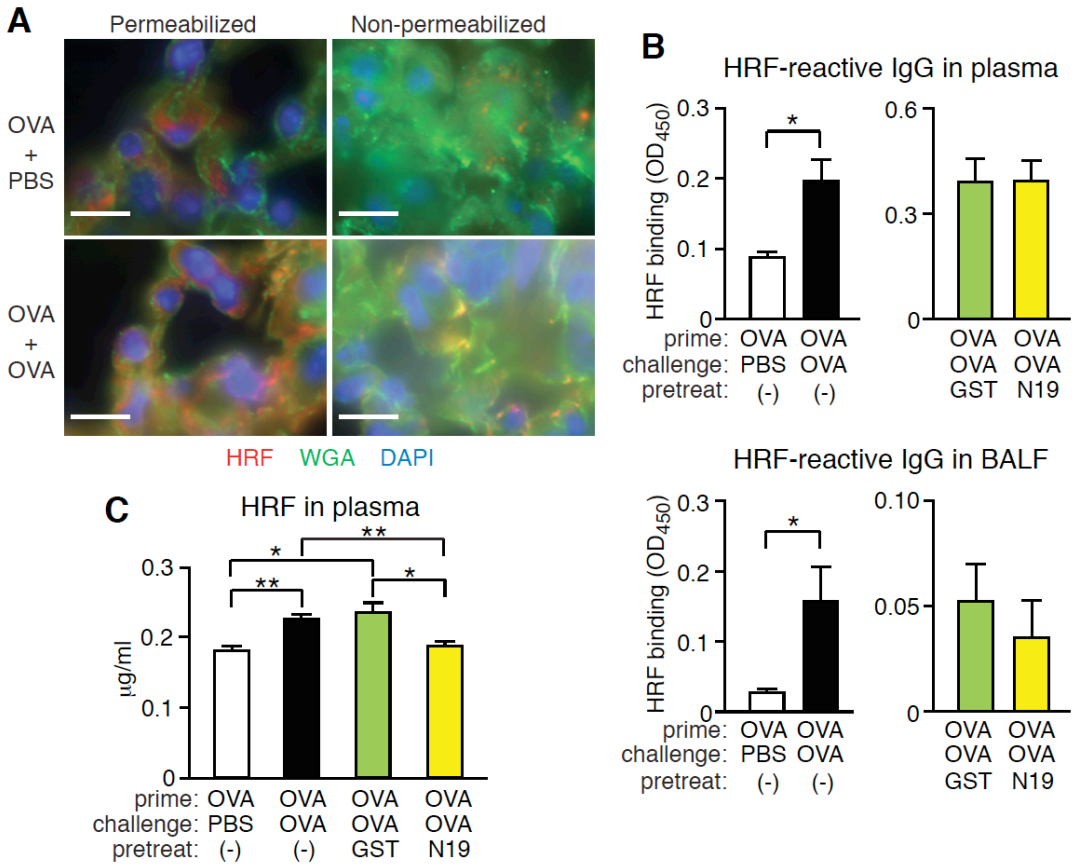

Figure S12. HRF is secreted in lung tissues and HRF levels, but HRF-reactive IgG levels are not reduced by GST-N19 in plasma and lungs in OVA-immunized and OVA-challenged mice. OVA-immunized mice were intranasally challenged with OVA or PBS, as described for **Figure 6**. Some mice were pretreated with GST or GST-N19 before each OVA challenge. Twenty four h after the last challenge, the mice were sacrificed and BAL fluids, plasma and lung tissues were collected. (**A**) Immunofluorescence microscopy was performed on membrane-permeabilized or non-permeabilized lung tissues. HRF was stained red. The plasma membrane was stained with wheat germ agglutinin (green) and the nuclei with DAPI (blue). Bar = 10 µm. (**B**) HRF-reactive IgG was measured by ELISA. (**C**) HRF in plasma was quantified by immunoblotting. Data represent mean ± SEM. *, **: $p<0.05$, $p<0.01$ by Student's t-test.

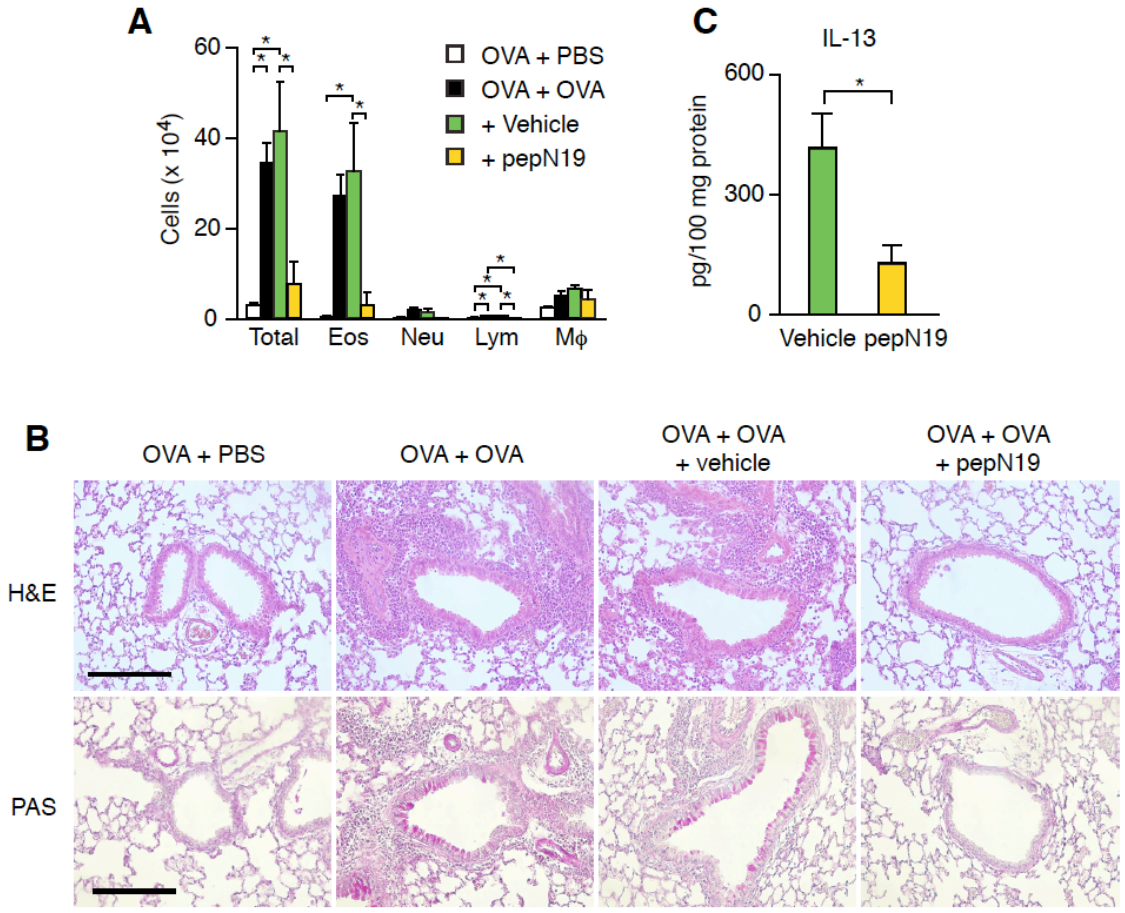

Figure S13. Synthetic N19 peptide inhibits airway inflammation. C57BL/6 mice were first sensitized with OVA (10 μg) on days 0, 7, 14, 21, 28, and 35. On days 40, 43 and 46, mice were intranasally challenged with OVA (20 μg) or PBS. Some mice were intranasally pretreated with 2% DMSO or synthetic N19 peptide (pepN19, 20 μg) before every OVA challenge. Twenty four h after the last challenge, mice were sacrificed and BAL fluids and lung tissues were collected. (**A**) Total and specific immune cell numbers in BAL fluids were enumerated. Eos, eosinophils; Neu, neutrophils; Lym, lymphocytes; Mϕ, macrophages. (**B**) Paraffin-embedded lung tissues were stained by H&E and periodic acid-Schiff (PAS). Bar = 200 μm. (**C**) IL-13 in lung homogenates was measured by ELISA. Data indicate mean ± SEM. *: $p<0.05$ by Student's t-test.

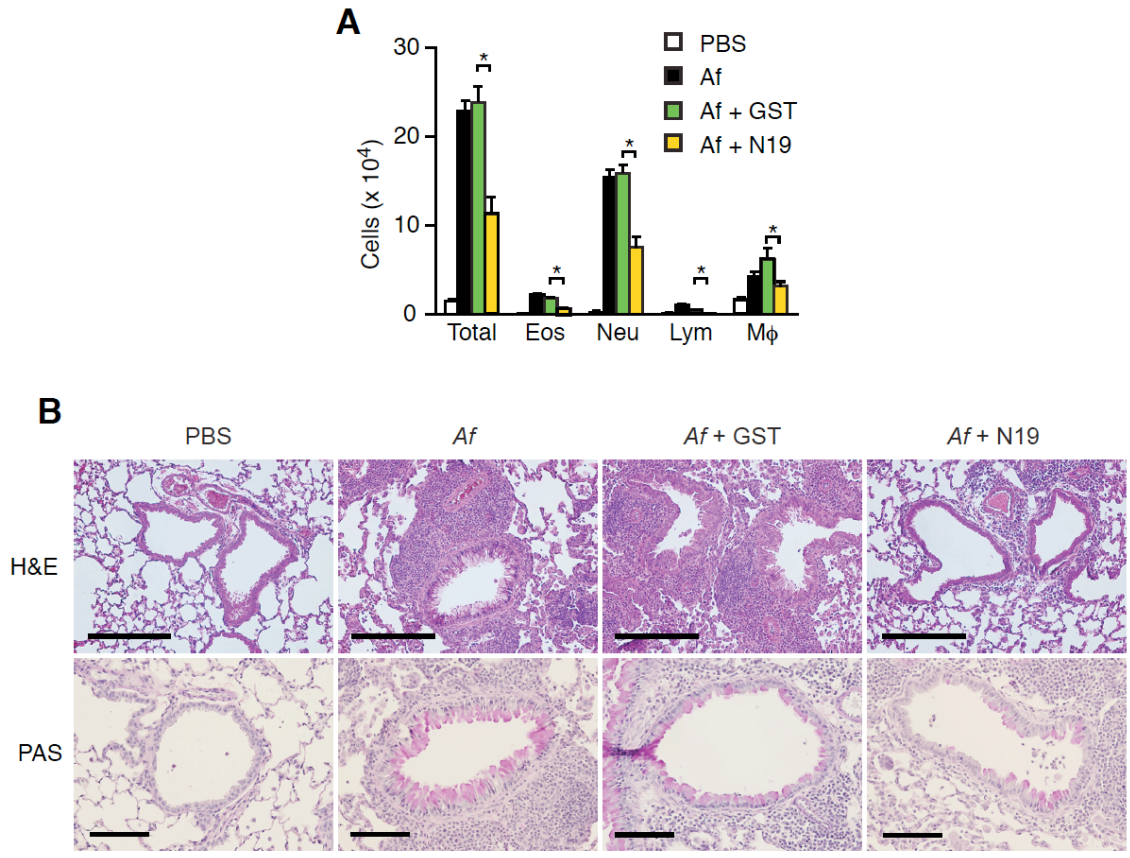

Figure S14. GST-N19 inhibits *Aspergillus fumigatus* allergen-induced airway inflammation. BALB/c mice were lightly anesthetized by isoflurane inhalation, and 50 μl of *Aspergillus* allergen or PBS was applied to the nares. Mice were immunized three times per week for 3 weeks, as described previously (2). Some mice were intranasally pretreated with GST or GST-N19 (200 μg/50 μl) from the second week 30 min before each immunization. Twenty four h after the last challenge, mice were sacrificed and BAL fluids and lung tissues were collected. 3-5 mice each cohort were used. Representative of 2 experiments. (**A**) Total and specific immune cell numbers in BAL fluids were enumerated. Eos, eosinophils; Neu, neutrophils; Lym, lymphocytes; Mϕ, macrophages. (**B**) Paraffin-embedded lung tissues were stained by H&E and periodic acid-Schiff (PAS). Bar = 100 μm. Data indicate mean ± SEM. *: $p<0.05$ by Student's t-test.

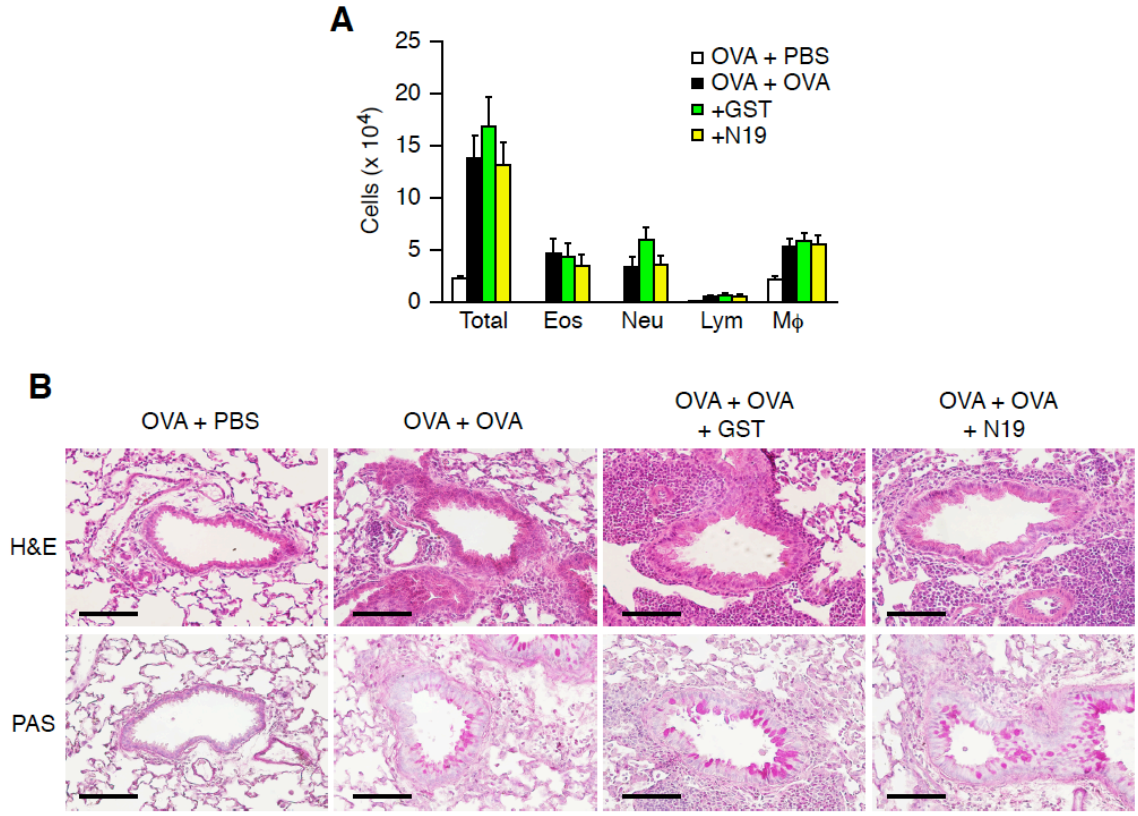

Figure S15. GST-N19 does not inhibit T cell-dependent but mast cell-independent airway inflammation. C57BL/6 mice were intraperitoneally immunized with OVA in the presence of alum on days 0 and 12. Mice were then lightly anesthetized by isoflurane inhalation, and intranasally administered with OVA (20 μg/20 μl) on days 24, 26, and 28. Some mice were intranasally pretreated with GST or GST-N19 (400 μg/20 μl) 15 min before each OVA challenge. Twenty four h after the last challenge, mice were sacrificed and BAL fluids and lung tissues were collected. (**A**) Total and specific immune cell numbers in BAL fluids were enumerated. Eos, eosinophils; Neu, neutrophils; Lym, lymphocytes; Mϕ, macrophages. (**B**) Paraffin-embedded lung tissues were stained by H&E and periodic acid-Schiff (PAS). Bar = 100 μm. Data indicate mean ± SEM.

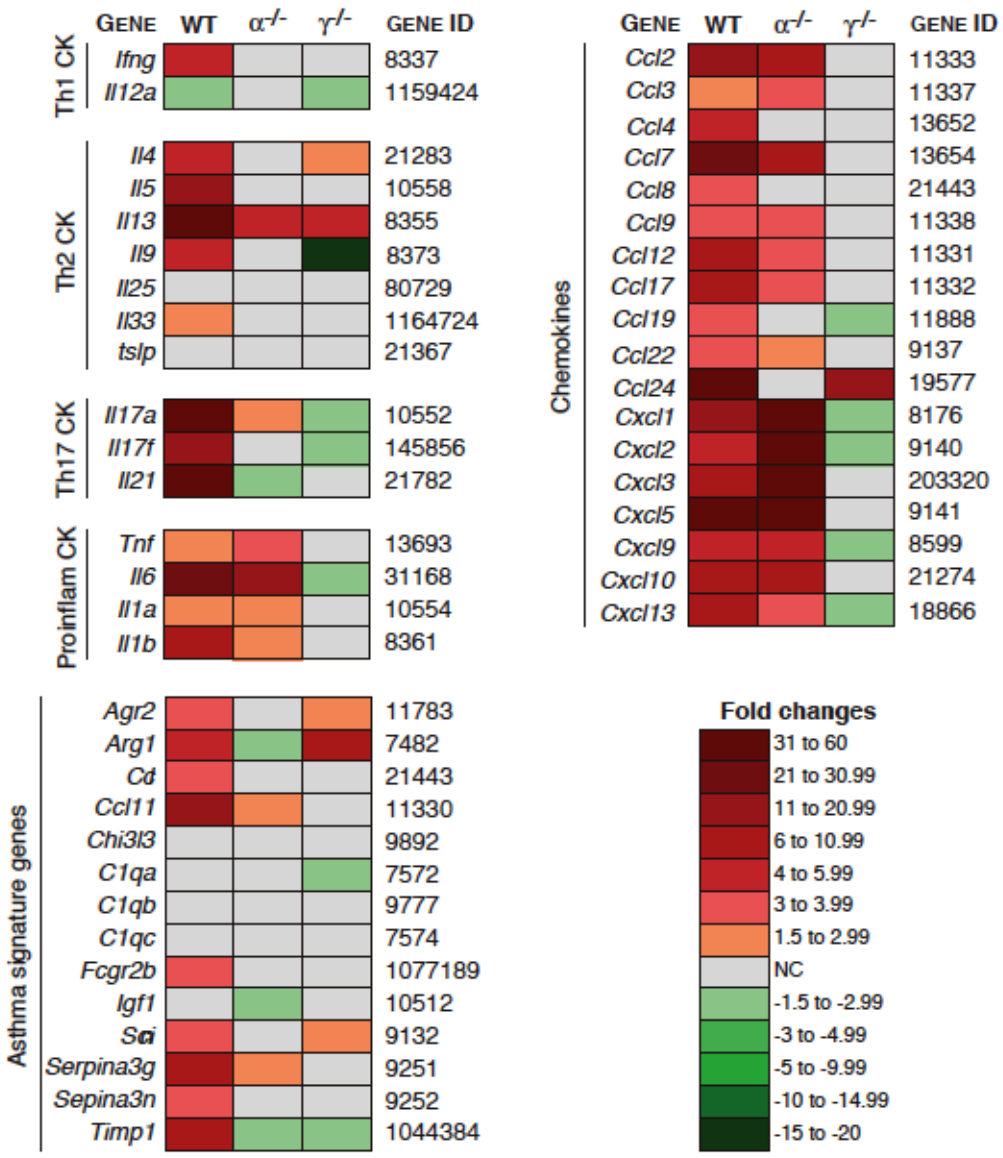

Figure S16. Expression of cytokines, chemokines and asthma signature genes is induced by HRF in the lungs. Naive C57BL/6 (WT), *FcεRIα*$^{-/-}$ and *FcRγ*$^{-/-}$ mice were treated intranasally with 40 μg mHRF-His_6 three times every third day. PBS served as a negative control. Lungs were isolated 24 h after the last treatment. RNAs were purified and subjected to microarray analysis. Fold expression by HRF-treated over PBS-treated mice was calculated. Heat map is shown for Th1-, Th2-, Th17-associated cytokines, chemokines and asthma signature genes. Chemokine genes whose expression was not altered >3 fold in any of the mice are omitted.

Supplementary Table 1. Usage of gene segments in IgE and IgG molecules

	VH	HD	HJ	VL	LJ
IgE					
AR40EA	1-28	1-1	4	8-30	2
BE2	7-3	4-1	3	8-30	2
SPE-7	1-72	1-1	2	1 (l)	1
H1 DNP-e-206	5-6	2-2	1	1-110	1
H1 DNP-e-26	5-6	2-2	1	3-12	2
BE1BD2D5	7-3	4-1	3	1-110	5
BE4C2C3	3-8	3-3	3	8-28	2
DNP48BC2	5-17	2-14	1	6-15	5
DNP48BD1IA4	5-6	3-3	2	6-32	4
HB30AIIA1C3	1-28	1-1	4	1-117	1
R25B4C1	5-17	5-2	2	6-32	2
TOE	1-63	2-2	2	3-12	2
IgG					
JK17	1-67	3-3	3	2-137	2
JK18	1-67	3-3	3	2-137	2
JK31	14-3	1-1	3	2-137	2
JK84	1-5	1-1	2	6-15	2
JK116	14-3	2-1	3	2-137	2
JK130	1-12	1-3	2	9-120	2
JK1	1-85	2-14	2	1	1
JK49	1-80	2-3	2	4-80	4
JK7	1-4	1-1	4	3-12	2
JKD4	9-3	1-1	3	4-55	5

Shown are gene family names coding for heavy chain variable (VH), diversity (HD), joining (HJ) regions and light chain variable (VL) and joining (LJ) regions. HRF-reactive IgEs and IgGs are indicated by bold font.

Supplementary Table 2. Primers used in this study

Forward primers for GST fusion proteins:

For N12, N19, N32, N47, N78, N142, N154 and full-length mHRF:

AAAAGGATCCATGATCATCTACCGGGACC

For N79-142 and N79-172:

AAAAGGATCCCAAGAAACCAGCTTCACAAA

For KYI-N16:

CCGGATCCAAGTACATCATGATCATCTACCGGGAC

Reverse primers for GST fusion proteins:

For N12: TTTGAATTCTTACTCGTCATGGCTGAT

For N19: AAAGAATTCTTACTTGTAGATGTCGGAGAACA

For N32: AAAGAATTCTTACTCCACCTCCAGGCACAGCC

For N47: AAAGAATTCTTAGAGCGAGTCATCGATGGCAC

For N78: AAAGAATTCTTATAAGTGATGGTTCATGACAA

For N142 and N79-142: AAAGAATTCTTATGGATTCATGTTTTCACCAA

For full-length and N79-172: AAAAGGATCCCAAGAAACCAGCTTCACAAA

Forward primer for His_6-tagged mHRF:

AAAACATATGATCATCTACCGGGACCT

Reverse primer for His_6-tagged mHRF:

TTTTCTCGAGACATTTCTCCATCTCTAAGC

Supplementary Table 3. Sources of IgEs and IgGs used in this study

IgE	
26 (H1 DNP-e-26), 206 (H1 DNP-e-206)	Fu-Tong Liu (UC Davis)
AR40EA, BE1BD (BE1BD2D5), BE2, BE4 (BE4C2C3), DNP48BC, DNP48BD, HB30, R25, TOE	Reuben P. Siraganian (NIH)
αOE	Erwin Gelfand (National Jewish Health)
C38-2, C48-2, 27-74	BD Biosciences
SPE-7	Sigma-Aldrich
IGELa2	ATCC
IgG	
164732, G115-178, JK series, MOPC-21, TT213-24	Kyowa Hakko Kirin California, Inc.
CD28.6, HIT3a, OKT3	eBioscience
2H11	Santa Cruz Biotechnology
5C3, A112-2, ACT35, RPA-T4, SP34	BD Pharmingen
MY31	BD Biosciences

References

1. Gould, H.J. & Sutton, B.J. IgE in allergy and asthma today. *Nat Rev Immunol* **8**, 205-217 (2008).
2. Mathias, C.B. *et al.* IgE influences the number and function of mature mast cells, but not progenitor recruitment in allergic pulmonary inflammation. *J Immunol* **182**, 2416-2424 (2009).